energies

MDPI

Article

Multi-Level Cooperative Scheduling Based on Robust Optimization Considering Flexibilities and Uncertainties of ADN and MG

Ziqi Zhang [1], Zhong Chen [1,*], Qi Zhao [2] and Puliang Du [1]

[1] School of Electrical Engineering, Southeast University, Nanjing 210096, China; zqzhang_ee@seu.edu.cn (Z.Z.); dupuliang@163.com (P.D.)
[2] Suzhou Power Supply Branch, State Grid Jiangsu Electric Power Co., Ltd., Suzhou 215004, China; zqsz2021@163.com
* Correspondence: chenzhong__seu@163.com

Abstract: This paper develops the coordination structure and method for utilizing flexibilities in a Micro-Grid (MG), an Active Distribution Network (ADN) and a Transmission Grid (TG), which can play an essential role in addressing the uncertainties caused by renewable energy power generation (REPG). For cooperative dispatching, both flexibilities and uncertainties on the interface of MG–ADN and ADN–TG are portrayed in unified forms utilizing robust optimization (RO), based on the modified equipment-level model of flexible resources. The Constraint-and-Column Generation method is adopted to solve the RO control problems. Simulations on the modified IEEE case-6 and case-33 systems are carried out. The results suggest that the proposed algorithm can exploit flexible resources in both an MG and an ADN, improving the economy and promoting REPG consumption within each level (MG, ADN and TG) while reducing uncertainties and providing flexibilities for superior operators.

Keywords: multi-level scheduling; robust optimization (RO); flexibility and uncertainty; renewable energy power generation

check for updates

Citation: Zhang, Z.; Chen, Z.; Zhao, Q.; Du, P. Multi-Level Cooperative Scheduling Based on Robust Optimization Considering Flexibilities and Uncertainties of ADN and MG. *Energies* **2021**, *14*, 7376. https://doi.org/10.3390/en14217376

Academic Editor: Nick Papanikolaou

Received: 12 October 2021
Accepted: 1 November 2021
Published: 5 November 2021

Publisher's Note: MDPI stays neutral with regard to jurisdictional claims in published maps and institutional affiliations.

Copyright: © 2021 by the authors. Licensee MDPI, Basel, Switzerland. This article is an open access article distributed under the terms and conditions of the Creative Commons Attribution (CC BY) license (https://creativecommons.org/licenses/by/4.0/).

1. Introduction

The continuous growth of renewable energy power generation (REPG) represented by wind power (WP) and photovoltaics (PV) is an important support for peaking carbon dioxide emissions before 2030 and achieving carbon neutrality [1]. REPGs are injecting into power systems at various levels, including a Micro-Grid (MG), an Active Distribution Network (ADN) and a Transmission Grid (TG), causing problems of multi-level scheduling for REPG consumption and economic operation [2,3].

Dealing with the uncertainties of REPG utilizing various kinds of flexible resources plays a significant role in improving REPG consumption and optimal operation, despite the different emphases of scheduling in multiple levels [4,5]. The scenario-based stochastic method used to be the most popular way to cope with the uncertainties in optimization. For optimal dispatching in an MG, the operating economy is generally the primary goal, which is frequently integrated with indicators related to reliability and the environment [6]. A stochastic model for the coordinated scheduling of renewable and thermal units, including fuel cell units and hydrogen storage, was proposed in [7]. A two-layer control scheme operating at two different timescales was illustrated in [8] for the energy management of an MG based on stochastic model predictive control. The main feature of optimal scheduling in an ADN compared to it in an MG is the necessity to handle the power flow, which can be nonlinear [9,10]. In studies [11,12], the high penetration of plug-in electric vehicles, demand response and energy storage were considered as flexible resources, and network loss was included in the optimization goals. For optimization in a TG, unit commitment is the key issue. Stochastic methods were adopted in [13–15] to comprise fluctuations of WP and load.

However, the scenario-based process requires the distributions of stochastic parameters, which might be difficult to obtain. On the contrary, robust optimization (RO) considers the worst-case has no need for a specific distribution. Therefore, many researchers have based their approaches on RO in recent years [16–18]. Sets or budgets of uncertainties are of great significance in RO problems. The point estimate method was applied in [19] for modeling the uncertainties budgets of WP and PV. A data-driven approach was employed in [20] to construct a more practical polyhedron uncertainty set for WP. However, the uncertainties of an ADN or an MG as a whole have not been investigated.

Vertical coordination provides various means for REPG consumption and economic improvement. The coordinated scheduling between a TG and an ADN or an ADN and an MG has gradually become a research hotspot. S. Bahramara et al. [21] proposed a hierarchical decision-making framework for the reduction in the cost of an ADN and an MG; however, the uncertainties were neglected. A decentralized algorithm was proposed to optimize an ADN and MGs independently in [22]; however, the uncertainties of MGs were not taken into consideration. The analytic target cascading (ATC) was applied in [23] to search the optimal dispatch strategy of a TG and an ADN; however, the uncertainties of REPGs in ADNs were ignored. In an investigation of comprehensive optimization for an MG and an ADN [24], a bi-level, two-stage RO model was established; however, the influence of ADNs' scheduling results on a TG was not investigated. To the best of the authors' knowledge, there have been few pieces of research about the tri-level collaborative scheduling of a TG, an ADN and an MG considering the uncertainties in different levels.

The studies discussed above have only focused on the optimal dispatching utilizing flexible resources directly. However, due to the independent interests of various subjects and information privacy, global optimization might be difficult to perform [25]. Therefore, quantitative characterizations of flexibilities in different levels are not only significant for superior optimization but also essential for defining the contribution of each participant. Several attempts have been made to quantify operational flexibility. An analytical framework for quantifying the flexibility of an ADN was proposed in [26,27], including the quantification of node flexibility, the matching of system flexibility and the flexibility of network transmission. An RO method based on the linearized load flow model was proposed in [28] to estimate the reserve provision capability area of an ADN. However, the applications of those flexibilities in optimized scheduling were not studied. A qualitative study in [29] described a model for defining and optimizing distributed energy flexibility in distribution buses available for the day-ahead energy market. However, the uncertainties of REPGs and other flexible resources were not considered. Since the resource endowments of participants in multi-level scheduling are fluctuant, at a particular moment, some participants can provide flexibilities while others may remain uncertain (which have demand for external flexibilities). However, very few studies have explored the unified model for flexibility supply/demand of different participants.

This paper provides new insights into optimal cooperative scheduling of an MG, an ADN and a TG. The main contributions are as follows:

1. Based on RO, considering equipment-level models, the flexibilities and uncertainties of MGs are uniformly expressed through the signs and magnitudes of the variables interacting with an ADN, allowing transactions for both power and flexibilities between an ADN and MGs.
2. Whether an ADN has flexibilities or uncertainties is determined utilizing RO methods. The power in the root node of an ADN will result in controllable intervals if the ADN has flexibilities. Otherwise, it will turn to uncertain budgets. This method provides convenience for a TG to perceive uncertainties and employ flexibilities of the ADN.
3. The Constraint-and-Column Generation (C&CG) method is chosen to solve the RO problems for reliability and efficiency.
4. To minimize the cost of flexibilities, a bi-level optimization of an MG and an ADN is developed based on a price adjustment mechanism.

The following arrangements are as follows: The second section constructs the overall framework for multi-level coordination. The third section proposes RO models for an MG, an ADN and a TG. The fourth section introduces the price adjustment mechanism for flexibilities and the solution method. Case studies based on typical scenarios are carried out in the fifth section. The final section summarizes the main findings of these experiments and provides a conclusion to the paper.

2. Framework for Multi-Level Scheduling

As shown in Figure 1, the multi-level coordination architecture is generally divided into three parts: an MG, an ADN and a TG (or sub-TG).

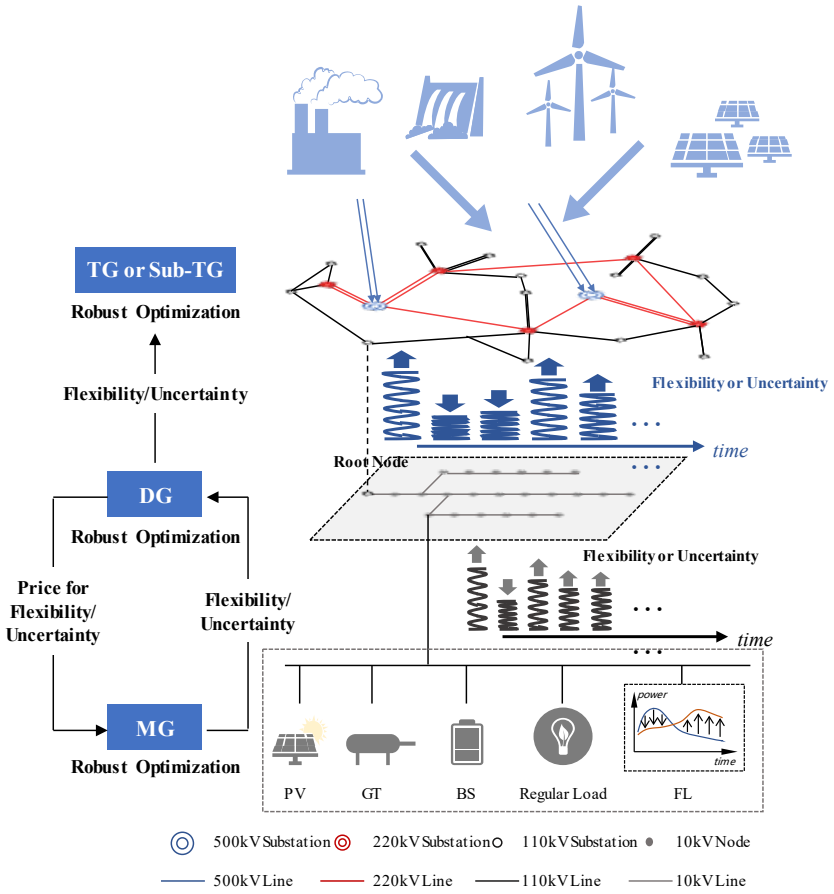


Figure 1. Framework for multi-level scheduling.

To begin the process, RO is carried out in the MG, considering the uncertainties of internal REPG and regular load (RL). The purpose is to exploit the flexibilities and reduce the uncertainties for the and, while the operating costs of the MG are cut down. After optimization, the intervals of flexibilities or uncertainties will be sent to the ADN. In addition, the flexibilities or uncertainties of multiple MGs cooperate with resources directly controlled by the ADN using RO, to optimize the controllability of power in the root node of the ADN. Modulations of price for flexibility/uncertainty are performed according to the optimization results before being fed back to MGs. Once the iteration has been completed, a flexible/uncertain range of power in the root node of the ADN will be reported to the TG. Finally, the TG utilizes flexibilities provided by ADNs and thermal power plants to deal with uncertainties, aiming at reducing the operating cost and promoting the consumption of REPG.

3. Optimization Models

The section below will propose RO models for the MG, ADN and TG. The number of time intervals is represented by T, and the length of each interval is donated by Δt.

3.1. MG

The optimization goal of the MG is as follows:

$$\min_{P_{i,t}^{\mathrm{MG,L}} \in \boldsymbol{P}_{i,t}^{\mathrm{MG,L}}, P_{i,t}^{\mathrm{MG,PV}} \in \boldsymbol{P}_{i,t}^{\mathrm{MG,PV}}} \sum_{t \in T} \Big[C_{i,t}^{\mathrm{MG,base}} p_{i,t}^{\mathrm{MG,base}} \Delta t + C_{i,t}^{\mathrm{MO,up}} p_{i,t}^{\mathrm{MO,up}} + C_{i,t}^{\mathrm{MO,down}} p_{i,t}^{\mathrm{MO,down}} + C_i^{\mathrm{MG,B}} \left(p_{i,t}^{\mathrm{MG,BC}} + p_{i,t}^{\mathrm{MG,BD}} \right) \Delta t + \left(C_i^{\mathrm{MG,GT}} p_{i,t}^{\mathrm{MG,GT}} \Delta t + B_i^{\mathrm{MG,GT}} u_{i,t}^{\mathrm{MG,GT}} \right) \Big] \tag{1}$$

where $C_{i,t}^{\mathrm{MG,base}}$ is the unit power purchase price for the MG i during time interval t, and $p_{i,t}^{\mathrm{MG,base}}$ is the power that the MG absorbs from the ADN. $p_{i,t}^{\mathrm{MO,up}}/p_{i,t}^{\mathrm{MO,down}}$ is the upward/downward flexible ramping product (FRP) purchased from or sold to the ADN, respectively, while $C_{i,t}^{\mathrm{MO,up}}/C_{i,t}^{\mathrm{MO,down}}$ are the unit prices. $p_{i,t}^{\mathrm{MG,BC}}/p_{i,t}^{\mathrm{MG,BD}}$ are the charge/discharge power of battery storage (BS) with unit cost $C_i^{\mathrm{MG,B}}$. $p_{i,t}^{\mathrm{MG,GT}}$ and $u_{i,t}^{\mathrm{MG,GT}}$ are the output power and operating status of GT, while $C_i^{\mathrm{MG,GT}}$ and $B_i^{\mathrm{MG,GT}}$ are separately the fixed and variable costs, respectively. $\boldsymbol{P}_{i,t}^{MG,L}$ and $\boldsymbol{P}_{i,t}^{MG,PV}$ represent the uncertain budgets of RL and the limitation of PV output, respectively.

Turning now to the constraints. The following formula reveals the power balance constraint of the MG considering flexibilities and uncertainties:

$$\begin{cases} p_{i,t}^{\mathrm{MG,base}} + p_{i,t}^{\mathrm{MG,up}} \geq P_{i,t}^{\mathrm{MG,L}} + p_{i,t}^{\mathrm{MG,FL}} + p_{i,t}^{\mathrm{MG,BC}} - p_{i,t}^{\mathrm{MG,PV}} - p_{i,t}^{\mathrm{MG,GT}} - p_{i,t}^{\mathrm{MG,BD}} \\ p_{i,t}^{\mathrm{MG,base}} - p_{i,t}^{\mathrm{MG,down}} \leq P_{i,t}^{\mathrm{MG,L}} + p_{i,t}^{\mathrm{MG,FL}} + p_{i,t}^{\mathrm{MG,BC}} - p_{i,t}^{\mathrm{MG,PV}} - p_{i,t}^{\mathrm{MG,GT}} - p_{i,t}^{\mathrm{MG,BD}} \\ p_{i,t}^{\mathrm{MG,up}} = p_{i,t}^{\mathrm{MI,up}} + p_{i,t}^{\mathrm{MO,up}} \\ p_{i,t}^{\mathrm{MG,down}} = p_{i,t}^{\mathrm{MI,down}} + p_{i,t}^{\mathrm{MO,down}} \\ p_{i,t}^{\mathrm{MG,up}}, p_{i,t}^{\mathrm{MG,down}} \geq 0 \end{cases} \tag{2}$$

where $P_{i,t}^{\mathrm{MG,L}}$ and $p_{i,t}^{\mathrm{MG,PV}}$ are the power of RL and PV, respectively, which are generated from the uncertain budgets. $p_{i,t}^{\mathrm{MG,FL}}$ represents the power of flexible load (FL). $p_{i,t}^{\mathrm{MG,up}}/p_{i,t}^{\mathrm{MG,down}}$ are the upward/downward FRPs that are necessary to cover the uncertainties of the MG i, while $p_{i,t}^{\mathrm{MI,up}}/p_{i,t}^{\mathrm{MI,down}}$ are FRPs that can be obtained inside this MG. As shown in Figure 2, when the internal flexibilities of the MG are sufficient to cover its uncertainties, the MG can sell superfluous flexibilities to the ADN and $p_{i,t}^{\mathrm{MO,up}}$ or $p_{i,t}^{\mathrm{MO,down}}$ is less than zero. On the contrary, it is necessary for the MG to purchase flexibilities from the ADN, and $p_{i,t}^{\mathrm{MO,up}}$ or $p_{i,t}^{\mathrm{MO,down}}$ is greater than zero.

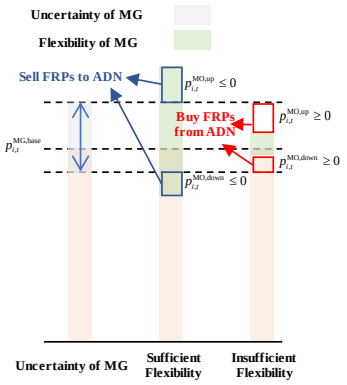


Figure 2. Power balance considering flexibility and uncertainty of MG.

The internal flexible resources of the MG consist of PV, BS, GT and FL.

$$\begin{cases} p_{i,t}^{\mathrm{MI,up}} = p_{i,t}^{\mathrm{MG,PV,up}} + p_{i,t}^{\mathrm{MG,B,up}} + p_{i,t}^{\mathrm{MG,GT,up}} + p_{i,t}^{\mathrm{MG,FL,up}} \\ p_{i,t}^{\mathrm{MI,down}} = p_{i,t}^{\mathrm{MG,PV,down}} + p_{i,t}^{\mathrm{MG,B,down}} + p_{i,t}^{\mathrm{MG,GT,down}} + p_{i,t}^{\mathrm{MG,FL,down}} \end{cases} \tag{3}$$

where $p_{i,t}^{\mathrm{MG,PV,up}}/p_{i,t}^{\mathrm{MG,PV,down}}$, $p_{i,t}^{\mathrm{MG,B,up}}/p_{i,t}^{\mathrm{MG,B,down}}$, $p_{i,t}^{\mathrm{MG,GT,up}}/p_{i,t}^{\mathrm{MG,GT,down}}$,$p_{i,t}^{\mathrm{MG,FL,up}}/p_{i,t}^{\mathrm{MG,FL,down}}$ refer to the upward/downward FRPs of PV, BS, GT and FL inside the MG i, respectively. The relevant constraints will be discussed in detail below.

- PV

PV can provide upward/downward FRPs by increasing/reducing the output power. However, it is restricted by the limitation of PV output.

$$\begin{cases} p_{i,t}^{\mathrm{MG,PV}} + p_{i,t}^{\mathrm{MG,PV,up}} \le \mathrm{P}_{i,t}^{\mathrm{MG,PV}} \\ p_{i,t}^{\mathrm{MG,PV}} - p_{i,t}^{\mathrm{MG,PV,down}} \ge 0 \\ p_{i,t}^{\mathrm{MG,PV,up}}, p_{i,t}^{\mathrm{MG,PV,down}} \ge 0 \end{cases} \tag{4}$$

- BS

FRPs can be exploited in BS by several means. Specifically, there are the following three ways to obtain an upward FRP: decrease the charging power, denoted as $p_{i,t}^{\mathrm{MG,BC,up1}}$; switch from a charging state to a discharging state, denoted as $p_{i,t}^{\mathrm{MG,BC,up2}}$; increase the discharging power, denoted as $p_{i,t}^{\mathrm{MG,BD,up3}}$. Similarly, there are also the following three ways to obtain a downward FRP: decrease the discharging power, denoted as $p_{i,t}^{\mathrm{MG,BD,down1}}$; switch from a discharging state to a charging state, denoted as $p_{i,t}^{\mathrm{MG,BD,down2}}$; increase the charging power, denoted as $p_{i,t}^{\mathrm{MG,BC,down3}}$. The constraints are as follows:

$$\begin{cases} u_{i,t}^{\mathrm{MG,BC}} + u_{i,t}^{\mathrm{MG,BD}} \le 1 \\ P_{i,\min}^{\mathrm{MG,BC}} u_{i,t}^{\mathrm{MG,BC}} \le p_{i,t}^{\mathrm{MG,BC}} \le P_{i,\max}^{\mathrm{MG,BC}} u_{i,t}^{\mathrm{MG,BC}} \\ P_{i,\min}^{\mathrm{MG,BD}} u_{i,t}^{\mathrm{MG,BD}} \le p_{i,t}^{\mathrm{MG,BD}} \le P_{i,\max}^{\mathrm{MG,BD}} u_{i,t}^{\mathrm{MG,BD}} \\ E_{i,t}^{\mathrm{MG,B,up}} = E_{i,t_0}^{\mathrm{MG,B}} + \sum_{j=1}^{t} \left[p_{i,j}^{\mathrm{MG,BC}} - p_{i,j}^{\mathrm{MG,BD}} \right] \Delta t - \sum_{j=1}^{t} p_{i,j}^{\mathrm{MG,B,up}} \Delta t \\ E_{i,\min}^{\mathrm{MG,B}} \le E_{i,t}^{\mathrm{MG,B,up}} \\ E_{i,t}^{\mathrm{MG,B,down}} = E_{i,t_0}^{\mathrm{MG,B}} + \sum_{j=1}^{t} \left[p_{i,j}^{\mathrm{MG,BC}} - p_{i,j}^{\mathrm{MG,BD}} \right] \Delta t + \sum_{j=1}^{t} p_{i,j}^{\mathrm{MG,B,down}} \Delta t \\ E_{i,\max}^{\mathrm{MG,B}} \ge E_{i,t}^{\mathrm{MG,B,down}} \\ p_{i,t}^{\mathrm{MG,B,up}} = p_{i,t}^{\mathrm{MG,BC,up1}} + p_{i,t}^{\mathrm{MG,BC,up2}} + p_{i,t}^{\mathrm{MG,BD,up3}} \\ p_{i,t}^{\mathrm{MG,B,down}} = p_{i,t}^{\mathrm{MG,BD,down1}} + p_{i,t}^{\mathrm{MG,BD,down2}} + p_{i,t}^{\mathrm{MG,BC,down3}} \end{cases} \tag{5}$$

where $u_{i,t}^{\mathrm{MG,BC}}/u_{i,t}^{\mathrm{MG,BD}}$ are 0–1 variables indicating the charging/discharging state of BS. $P_{i,\min}^{\mathrm{MG,BC}}/P_{i,\min}^{\mathrm{MG,BD}}$ and $P_{i,\max}^{\mathrm{MG,BC}}/P_{i,\max}^{\mathrm{MG,BD}}$ are the minimum and maximum power of BS charging/discharging, respectively. $E_{i,t_0}^{\mathrm{MG,B}}$ represents energy in BS at the initial moment. In general, providing an upward FRP results in a decrease in BS energy; therefore, $E_{i,t}^{\mathrm{MG,B,up}}$ considering upward flexibility should be limited to greater than $E_{i,\min}^{\mathrm{MG,B}}$, the minimum energy of BS and vice versa.

As discussed above, an upward FRP of BS consists of $p_{i,t}^{\mathrm{MG,BC,up1}}$,$p_{i,t}^{\mathrm{MG,BC,up2}}$ and $p_{i,t}^{\mathrm{MG,BD,up3}}$, which can be depicted by the following formula:

$$\begin{cases} 0 \le p_{i,t}^{\mathrm{MG,BC,up1}} \le p_{i,t}^{\mathrm{MG,BC}} - P_{i,\min}^{\mathrm{MG,BC}} u_{i,t}^{\mathrm{MG,BC}} \\ p_{i,t}^{\mathrm{MG,BC,up1}} \le \left(P_{i,\max}^{\mathrm{MG,BC}} - P_{i,\min}^{\mathrm{MG,BC}}\right)\left(1 - s_{i,t}^{\mathrm{MG,BCD}}\right) \\ s_{i,t}^{\mathrm{MG,BCD}} \le u_{i,t}^{\mathrm{MG,BC}} \\ s_{i,t}^{\mathrm{MG,BCD}}\left(p_{i,t}^{\mathrm{MG,BC}} + P_{i,\min}^{\mathrm{MG,BD}}\right) \le p_{i,t}^{\mathrm{MG,BC,up2}} \le s_{i,t}^{\mathrm{MG,BCD}}\left(p_{i,t}^{\mathrm{MG,BC}} + P_{i,\max}^{\mathrm{MG,BD}}\right) \\ 0 \le p_{i,t}^{\mathrm{MG,BD,up3}} \le P_{i,\max}^{\mathrm{MG,BD}} u_{i,t}^{\mathrm{MG,BD}} - p_{i,t}^{\mathrm{MG,BD}} \end{cases} \tag{6}$$

where $s_{i,t}^{\mathrm{MG,BCD}}$ are 0–1 variables. When $s_{i,t}^{\mathrm{MG,BDC}} = 1$, the BS is switched from a charging state to a discharging state. Otherwise, its state remains.

A downward FRP of BS can be modeled in the same way:

$$\begin{cases} 0 \le p_{i,t}^{\mathrm{MG,BD,down1}} \le p_{i,t}^{\mathrm{MG,BD}} - P_{i,\min}^{\mathrm{MG,BD}} u_{i,t}^{\mathrm{MG,BD}} \\ p_{i,t}^{\mathrm{MG,BC,down1}} \le \left(P_{i,\max}^{\mathrm{MG,BD}} - P_{i,\min}^{\mathrm{MG,BD}}\right)\left(1 - s_{i,t}^{\mathrm{MG,BDC}}\right) \\ s_{i,t}^{\mathrm{MG,BDC}} \le u_{i,t}^{\mathrm{MG,BD}} \\ s_{i,t}^{\mathrm{MG,BDC}}\left(p_{i,t}^{\mathrm{MG,BD}} + P_{i,\min}^{\mathrm{MG,BC}}\right) \le p_{i,t}^{\mathrm{MG,BD,down2}} \le s_{i,t}^{\mathrm{MG,BDC}}\left(p_{i,t}^{\mathrm{MG,BD}} + P_{i,\max}^{\mathrm{MG,BC}}\right) \\ 0 \le p_{i,t}^{\mathrm{MG,BC,down3}} \le P_{i,\max}^{\mathrm{MG,BC}} u_{i,t}^{\mathrm{MG,BC}} - p_{i,t}^{\mathrm{MG,BC}} \end{cases} \tag{7}$$

where $s_{i,t}^{\mathrm{MG,BDC}}$ are 0–1 variables, suggesting whether the state of BS is changed.

- GT

The following is the modified constraints of GT considering the flexibility. $u_{i,t}^{\mathrm{MG,GT}}$ are 0–1 variables describing the off/on state of GT. $P_{i,\max}^{\mathrm{MG,GT}}/P_{i,\min}^{\mathrm{MG,GT}}$ are the maximum/minimum operating power and $\Delta P_i^{\mathrm{MG,GT}}$ is the limitation of power change between time intervals.

$$\begin{cases} p_{i,t}^{\mathrm{MG,GT,up}}, p_{i,t}^{\mathrm{MG,GT,down}} \ge 0 \\ p_{i,t}^{\mathrm{MG,GT}} + p_{i,t}^{\mathrm{MG,GT,up}} \le P_{i,\max}^{\mathrm{MG,GT}} u_{i,t}^{\mathrm{MG,GT}}, t \in \{1,2,\cdots,T\} \\ P_{i,\min}^{\mathrm{MG,GT}} u_{i,t}^{\mathrm{MG,GT}} \le p_{i,t}^{\mathrm{MG,GT}} - p_{i,t}^{\mathrm{MG,GT,down}}, t \in \{1,2,\cdots,T\} \\ \left(p_{i,t+1}^{\mathrm{MG,GT}} + p_{i,t+1}^{\mathrm{MG,GT,up}}\right) - \left(p_{i,t}^{\mathrm{MG,GT}} - p_{i,t}^{\mathrm{MG,GT,down}}\right) \le \Delta P_i^{\mathrm{MG,GT}},\ t \in \{1,2,\cdots,T-1\} \\ \left(p_{i,t+1}^{\mathrm{MG,GT}} - p_{i,t+1}^{\mathrm{MG,GT,down}}\right) - \left(p_{i,t}^{\mathrm{MG,GT}} + p_{i,t}^{\mathrm{MG,GT,up}}\right) \ge -\Delta P_i^{\mathrm{MG,GT}},\ t \in \{1,2,\cdots,T-1\} \end{cases} \tag{8}$$

The constraints on GT off/on time are as follows:

$$\begin{cases} \sum\limits_{k=t}^{t+T_{i,\mathrm{run,min}}^{\mathrm{MG,GT}}-1} u_{i,k}^{\mathrm{MG,GT}} \ge T_{i,\mathrm{run,min}}^{\mathrm{MG,GT}}\left(u_{i,t}^{\mathrm{MG,GT}} - u_{i,t-1}^{\mathrm{MG,GT}}\right),\ t \in \left\{1,2,\cdots,T - T_{i,\mathrm{run,min}}^{\mathrm{MG,GT}} + 1\right\} \\ \sum\limits_{k=t}^{T} u_{i,k}^{\mathrm{MG,GT}} \ge (T-t+1)\left(u_{i,t}^{\mathrm{MG,GT}} - u_{i,t-1}^{\mathrm{MG,GT}}\right),\ t \in \left\{T - T_{i,\mathrm{run,min}}^{\mathrm{MG,GT}} + 2,\cdots,T\right\} \\ \sum\limits_{k=t}^{t+T_{i,\mathrm{down,min}}^{\mathrm{MG,GT}}-1}\left(1 - u_{i,k}^{\mathrm{MG,GT}}\right) \ge T_{i,\mathrm{down,min}}^{\mathrm{MG,GT}}\left(u_{i,t-1}^{\mathrm{MG,GT}} - u_{i,t}^{\mathrm{MG,GT}}\right),\ t \in \left\{1,2,\cdots,T - T_{i,\mathrm{down,min}}^{\mathrm{MG,GT}} + 1\right\} \\ \sum\limits_{k=t}^{T}\left(1 - u_{i,k}^{\mathrm{MG,GT}}\right) \ge (T-t+1)\left(u_{i,t-1}^{\mathrm{MG,GT}} - u_{i,t}^{\mathrm{MG,GT}}\right), t \in \left\{T - T_{i,\mathrm{down,min}}^{\mathrm{MG,GT}} + 2,\cdots,T\right\} \end{cases} \tag{9}$$

where $T_{i,\mathrm{down,min}}^{\mathrm{MG,GT}}/T_{i,\mathrm{run,min}}^{\mathrm{MG,GT}}$ are the minimum off/on times of GT.

- FL

Three kinds of FLs are examined in this paper, including transferable load, interruptible load and reducible load [30]. The constraints are discussed below.

Firstly, the transferable load cannot be interrupted once it is started. However, the integral working time can be advanced or delayed, as follows:

$$\begin{cases} \sum_{t'=t}^{t+T_i^{\mathrm{MG,FL,a}}-1} u_{i,t'}^{\mathrm{MG,FL,a}} \geq s_{i,t}^{\mathrm{MG,FL,a}} T_i^{\mathrm{MG,FL,a}}, t \in \left[\alpha_i^{\mathrm{MG,FL,a}}, \beta_i^{\mathrm{MG,FL,a}}\right] \\ \sum_{t=\alpha_i^{\mathrm{MG,FL,a}}}^{\beta_i^{\mathrm{MG,FL,a}}} u_{i,t}^{\mathrm{MG,FL,a}} = T_i^{\mathrm{MG,FL,a}} \\ \sum_{t=\alpha_i^{\mathrm{MG,FL,a}}}^{\beta_i^{\mathrm{MG,FL,a}}} s_{i,t}^{\mathrm{MG,FL,a}} = 1 \\ p_{i,t}^{\mathrm{MG,FL,a}} = u_{i,t}^{\mathrm{MG,FL,a}} P_{i,t}^{\mathrm{MG,FL,a}} \end{cases} \tag{10}$$

where $u_{i,t}^{\mathrm{MG,FL,a}}$ and $s_{i,t}^{\mathrm{MG,FL,a}}$ are both 0–1 variables, which are separately the operating and starting state of transferable load belonging to the MG i, respectively. $[\alpha_i^{\mathrm{MG,FL,a}}, \beta_i^{\mathrm{MG,FL,a}}]$ is the time range acceptable for the user. $P_{i,t}^{\mathrm{MG,FL,a}}$ represents the running power. Since the transferable load is disabled to adjust power continuously, it is not employed to provide an FRP.

Secondly, the interruptible load of which power can be regulated only has requirements for cumulative absorbed energy during the acceptable time range $[\alpha_i^{\mathrm{MG,FL,b}}, \beta_i^{\mathrm{MG,FL,b}}]$. In Formula (11), $p_{i,t}^{\mathrm{MG,FL,b}}$ represents the power value to be determined. The interruptible load provides upward/downward FRPs through a decreasing/increasing running power. The total energy absorbed during the schedulable period would be restricted to more/less than the minimum/maximum value $E_{i,\min}^{\mathrm{MG,FL,b}}/E_{i,\max}^{\mathrm{MG,FL,b}}$ if upward/downward FRPs were provided.

$$\begin{cases} p_{i,t}^{\mathrm{MG,FL,b}} + p_{i,t}^{\mathrm{MG,FL,b,down}} \leq P_{i,\max}^{\mathrm{MG,FL,b}} u_{i,t}^{\mathrm{MG,FL,b}} \\ p_{i,t}^{\mathrm{MG,FL,b}} - p_{i,t}^{\mathrm{MG,FL,b,up}} \geq P_{i,\min}^{\mathrm{MG,FL,b}} u_{i,t}^{\mathrm{MG,FL,b}} \\ p_{i,t}^{\mathrm{MG,FL,b,down}}, p_{i,t}^{\mathrm{MG,FL,b,up}} \geq 0 \\ \sum_{t=\alpha_i^{\mathrm{MG,FL,b}}}^{\beta_i^{\mathrm{MG,FL,b}}} \left(p_{i,t}^{\mathrm{MG,FL,b}} + p_{i,t}^{\mathrm{MG,FL,b,down}}\right)\Delta t \leq E_{i,\max}^{\mathrm{MG,FL,b}} \\ \sum_{t=\alpha_i^{\mathrm{MG,FL,b}}}^{\beta_i^{\mathrm{MG,FL,b}}} \left(p_{i,t}^{\mathrm{MG,FL,b}} - p_{i,t}^{\mathrm{MG,FL,b,up}}\right)\Delta t \geq E_{i,\min}^{\mathrm{MG,FL,b}} \end{cases} \tag{11}$$

Thirdly, the reducible loads running power is adjustable, but the operating time cannot be changed. It is supposed to have n_c discrete operating points, $P_{i,1}^{\mathrm{MG,FL,c}} \leq P_{i,2}^{\mathrm{MG,FL,c}} \leq \cdots \leq P_{i,n_c}^{\mathrm{MG,FL,c}}$. The schedulable time interval is from $\alpha_i^{\mathrm{MG,FL,c}}$ to $\beta_i^{\mathrm{MG,FL,c}}$ and $p_{i,t}^{\mathrm{MG,FL,c}}$ is the power value to be determined. The constraints are as follows:

$$\begin{cases} \sum_{h=1}^{n_c} u_{i,t,h}^{\mathrm{MG,FL,c}} = 1, t \in \left[\alpha_i^{\mathrm{MG,FL,c}}, \beta_i^{\mathrm{MG,FL,c}}\right] \\ p_{i,t}^{\mathrm{MG,FL,c}} = \sum_{k=1}^{n_c} u_{i,t,h}^{\mathrm{MG,FL,c}} P_{i,h}^{\mathrm{MG,FL,c}} \\ p_{i,t}^{\mathrm{MG,FL,c,up}} = p_{i,t}^{\mathrm{MG,FL,c}} - P_{i,1}^{\mathrm{MG,FL,c}} \\ p_{i,t}^{\mathrm{MG,FL,c,down}} = P_{i,n_c}^{\mathrm{MG,FL,c}} - p_{i,t}^{\mathrm{MG,FL,c}} \end{cases} \tag{12}$$

where $u_{i,t,w}^{\mathrm{MG,FL,c}}$ are 0–1 variables, indicating the operating points in the time period t. $p_{i,t}^{\mathrm{MG,FL,c,up}}/p_{i,t}^{\mathrm{MG,FL,c,down}}$ are upward/ downward FRPs of a reducible load in the MG i.

To sum up, the running power and FRP of FL can be described in the following formula:

$$\begin{cases} \sum_{h=1}^{n_c} u_{i,t,h}^{\mathrm{MG,FL,c}} = 1, t \in \left[\alpha_i^{\mathrm{MG,FL,c}}, \beta_i^{\mathrm{MG,FL,c}}\right] \\ p_{i,t}^{\mathrm{MG,FL,c}} = \sum_{k=1}^{n_c} u_{i,t,h}^{\mathrm{MG,FL,c}} P_{i,h}^{\mathrm{MG,FL,c}} \\ p_{i,t}^{\mathrm{MG,FL,c,up}} = p_{i,t}^{\mathrm{MG,FL,c}} - P_{i,1}^{\mathrm{MG,FL,c}} \\ p_{i,t}^{\mathrm{MG,FL,c,down}} = P_{i,n_c}^{\mathrm{MG,FL,c}} - p_{i,t}^{\mathrm{MG,FL,c}} \end{cases} \tag{13}$$

3.2. ADN

3.2.1. Parameters and Variables from MG

In the RO of the ADN, the absorbed power values of the MG, which purchases an FRP from the ADN, are regarded as uncertain parameters. In contrast, the power values of the MG, which sells an FRP to the ADN, are treated as control variables. As shown below, four conditions can be categorized according to $p_{i,t}^{\mathrm{MO,up}}$ and $p_{i,t}^{\mathrm{MO,down}}$ uploaded by the MG.

- $p_{i,t}^{\mathrm{MO,up}} < 0$ and $p_{i,t}^{\mathrm{MO,down}} < 0$

The internal flexible resources of the MG i are sufficient to cover its uncertainties, and the spare flexibilities are sold to the ADN. The power values $p_{j,t}^{\mathrm{MG}}$ of the MG i are seen as control variables that satisfy the following constraints:

$$p_{i,t}^{\mathrm{MG,base}} + p_{i,t}^{\mathrm{MO,up}} \le p_{j,t}^{\mathrm{MG}} \le p_{i,t}^{\mathrm{MG,base}} - p_{i,t}^{\mathrm{MO,down}} \tag{14}$$

where j is the node number of the ADN to which the MG i is connected.

- $p_{i,t}^{\mathrm{MO,up}} \ge 0$ and $p_{i,t}^{\mathrm{MO,down}} \ge 0$

Under this condition, the MG i fails to handle uncertainties itself and needs to achieve an FRP from the ADN. $p_{j,t}^{\mathrm{MG}}$ is considered as an uncertain parameter, which belongs to the uncertain set $P_{j,t}^{\mathrm{MG}} = [p_{i,t}^{\mathrm{MG,base}} - p_{i,t}^{\mathrm{MO,down}}, p_{i,t}^{\mathrm{MG,base}} + p_{i,t}^{\mathrm{MO,up}}]$.

- $p_{i,t}^{\mathrm{MO,up}} < 0$ and $p_{i,t}^{\mathrm{MO,down}} \ge 0$

In this case, the MG i has both flexibilities and uncertainties towards the ADN. It sells an upward FRP to the and, while it buys a downward FRP from the ADN. $P_{j,t}^{\mathrm{MG}}$ meets the following constraints:

$$P_{j,t}^{\mathrm{MG}} + p_{j,t}^{\mathrm{MO,up}} \le p_{j,t}^{\mathrm{MG}} \le P_{j,t}^{\mathrm{MG}}, P_{j,t}^{\mathrm{MG}} \in \left[p_{i,t}^{\mathrm{MG,base}} - p_{i,t}^{\mathrm{MO,down}}, p_{i,t}^{\mathrm{MG,base}}\right] \tag{15}$$

- $p_{i,t}^{\mathrm{MO,up}} \ge 0$ and $p_{i,t}^{\mathrm{MO,down}} < 0$

It is similar to case c. However, the MG i sells a downward FRP to the and, while it buys an upward FRP from the ADN:

$$P_{j,t}^{\mathrm{MG}} \le p_{j,t}^{\mathrm{MG}} \le P_{j,t}^{\mathrm{MG}} - p_{j,t}^{\mathrm{MO,down}}, P_{j,t}^{MG} \in \left[p_{i,t}^{\mathrm{MG,base}}, p_{i,t}^{\mathrm{MG,base}} + p_{i,t}^{\mathrm{MO,up}}\right] \tag{16}$$

3.2.2. Power Flow and Other Constraints

Power flow constraints can be relaxed based on second-order cone programming (SOCP), of which validity has been demonstrated in [9]. The power flow constraints in the standard form of SOCP are as follows, and the subscript t is omitted for brevity:

$$\begin{cases} \sum\limits_{j\in u(k)}\left(P_{jk}-L_{jk}R_{jk}\right)+P_k=\sum\limits_{l\in v(k)}P_{kl} \\ \sum\limits_{j\in u(k)}\left(Q_{jk}-L_{jk}X_{jk}\right)+Q_k=\sum\limits_{l\in v(k)}Q_{kl} \\ U_k=U_j-2\left(R_{jk}P_{jk}+X_{jk}Q_{jk}\right)+\left(\left(R_{jk}\right)^2+\left(X_{jk}\right)^2\right)L_{jk} \\ \left\| \begin{array}{c} 2P_{jk} \\ 2Q_{jk} \\ L_{jk}-U_j \end{array} \right\|_2 \le L_k+U_j \end{cases} \tag{17}$$

where j, k and l are the node numbers of the ADN. P_{jk} and Q_{jk} are the active and reactive power at the head of branch jk. R_{jk} and X_{jk} refer to the resistance and reactance of branch jk, respectively. P_k/Q_k are the injection of active/reactive power in node k. $u(k)$ is defined as the set of head nodes, of which branches end at k. Similarly, $v(k)$ is the set of end nodes, of which branches start at k. U_j is used to describe the square of voltage amplitude in node j, while L_{jk} represents the square of current amplitude in branch jk.

The safety constraints of node voltage and branch current are as follows:

$$\begin{cases} \left(V_j^{\min}\right)^2 \le U_{j,t} \le \left(V_j^{\max}\right)^2 \\ L_{jk,t} \le \left(I_{jk}^{\max}\right)^2 \end{cases} \tag{18}$$

Suppose the ADN is equipped with continuous reactive power compensation devices, the corresponding constraints are as follows:

$$Q_{j,\min}^{\text{com}} \le Q_{j,t}^{\text{com}} \le Q_{j,\max}^{\text{com}} \tag{19}$$

where $Q_{i,\min}^{\text{com}}/Q_{i,\max}^{\text{com}}$ are the minimum/maximum reactive power of compensation device in node j.

For the nodes to which MGs are connected, the injected power is as follows:

$$\begin{cases} P_{j,t}=-p_{j,t}^{\text{MG}} \\ Q_{j,t}=-p_{j,t}^{\text{MG}}\tan\varphi_j+Q_{j,t}^{\text{com}} \end{cases} \tag{20}$$

where φ_j is the power factor angle. RL, FL, GT, BS and PV directly regulated by the ADN have the same constraints as the corresponding elements in the MG; therefore, they will not be a repeat.

3.2.3. Optimization Objectives and Criteria for Flexibilities

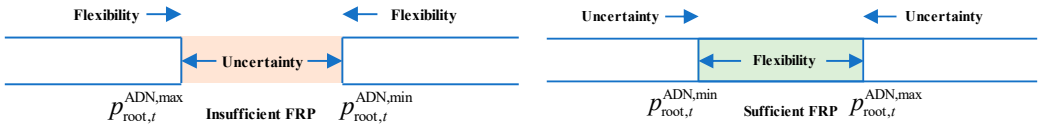
Since the ADN generally has a radial structure, it usually affects the TG through the power of its root node, $p_{\text{root},t}^{\text{ADN}}$. The number of ADNs is ignored for simplicity. Following the idea of RO, this paper intends to propose the criterion for flexibility/uncertainty of the ADN based on the following two optimizations:

$$\max_{p^{\text{P,ADN}}\in P^{\text{P,ADN}}}\left[\omega_m\sum_{t\in T}p_{\text{root},t}^{\text{ADN}}+(1-\omega_m)\sum_{t\in T}\sum_{j\in N_{\text{bus}}}\sum_{k\in v(j)}R_{jk}L_{jk,t}\right] \tag{21}$$

$$\min_{p^{\text{ADN}}\in P^{\text{ADN}}}\left[\omega_m\sum_{t\in T}p_{\text{root},t}^{\text{ADN}}-(1-\omega_m)\sum_{t\in T}\sum_{j\in N_{\text{bus}}}\sum_{k\in v(j)}R_{jk}L_{jk,t}\right] \tag{22}$$

where $p^{\mathrm{P,\,ADN}}$ and $\boldsymbol{P}^{\mathrm{P,\,ADN}}$ are uncertain parameters and their collections in the ADN, respectively. The weight coefficient ω_m will decrease with iteration, to ensure convergence. The goal of (21) is to find the robust minimum value of $p_{\mathrm{root},t}^{\mathrm{ADN}}$ considering the network loss, while (22) is to find the robust maximum value.

Since RO premeditates the degradation of the result owing to uncertainties, the solutions of (21) and (22) may appear in the following two situations, as shown in Figure 3.



(**a**) insufficient FRP (**b**) sufficient FRP

Figure 3. Different solutions of root node power Using RO.

- $p_{\mathrm{root},t}^{\mathrm{ADN,max}} < p_{\mathrm{root},t}^{\mathrm{ADN,min}}$

Uncertainties will cause the degradation of the optimization results, in other words, make the maximum value smaller but the minimum value larger. However, RO takes this degradation into account and adopts flexible resources to counteract it; therefore, the robust solution is stable and controllable. If the robust maximum value $p_{\mathrm{root},t}^{\mathrm{ADN,max}}$ is less than the robust minimum value $p_{\mathrm{root},t}^{\mathrm{ADN,min}}$, as shown in Figure 3a, the flexible resources inside the ADN are not enough to cover its uncertainties. As a result, $p_{\mathrm{root},t}^{\mathrm{ADN}}$, the power of the ADN is supposed to be an uncertain parameter that belongs to $\left[p_{\mathrm{root},t}^{\mathrm{ADN,max}}, p_{\mathrm{root},t}^{\mathrm{ADN,min}}\right]$ for the TG.

- $p_{\mathrm{root},t}^{\mathrm{ADN,max}} \geq p_{\mathrm{root},t}^{\mathrm{ADN,min}}$

As shown in Figure 3b, in this case, the internal flexible resources of the ADN can overcome its uncertainties. Therefore, the power of the ADN can be treated as a control variable by the TG, and the controllable interval is $\left[p_{\mathrm{root},t}^{\mathrm{ADN,min}}, p_{\mathrm{root},t}^{\mathrm{ADN,max}}\right]$.

To sum up, $P_t^{\mathrm{ADN,\,F}} = p_{\mathrm{root},t}^{\mathrm{ADN,max}} - p_{\mathrm{root},t}^{\mathrm{ADN,min}}$ is defined as the flexibility of the ADN. The flexibility rises with the $P_t^{\mathrm{ADN,\,F}}$. If $P_t^{\mathrm{ADN,\,F}} \geq 0$, the ADN has a flexible adjustment range for the TG. On the contrary, the ADN has uncertainty toward the TG when $P_t^{\mathrm{ADN,\,F}} < 0$.

3.3. TG

As discussed above, flexibilities/uncertainties due to RL, REPG, BS, etc., are integrated into unified expressions in the root node of the ADN (interface with the TG). Regarding optimization in the TG, a unit commitment is carried out considering the flexibilities/uncertainties of ADNs and concentrated REPGs (represented by WP).

3.3.1. Optimization Goal

The objective of unit commitment is to minimize both the power generation cost C_{G} and the reserve cost C_{R} as follows:

$$\begin{aligned} &\min_{p^{\mathrm{wind}} \in P^{\mathrm{wind}}, p^{\mathrm{ADN}} \in P^{\mathrm{ADN}}} C_{\mathrm{T}} = C_{\mathrm{G}} + C_{\mathrm{R}} \\ &C_{\mathrm{G}} = \sum_{t \in T} \sum_{g \in G} \left(k_g^0 + k_g^1 P_{g,t}^{\mathrm{G}} \Delta t + k_g^2 \left(P_{g,t}^{\mathrm{G}} \Delta t \right)^2 \right) \\ &C_{\mathrm{R}} = \sum_{t \in T} \sum_{g \in G} \left(q_g^{\mathrm{U}} R_{g,t}^{\mathrm{U}} + q_g^{\mathrm{D}} R_{g,t}^{\mathrm{D}} \right) \end{aligned} \tag{23}$$

where $\boldsymbol{P}^{\mathrm{wind}}$ is the uncertain set for output power of WP and $\boldsymbol{P}^{\mathrm{ADN}}$ is the uncertain set for the ADN. G is the number of the thermal generators and $P_{g,t}^{\mathrm{G}}$ is the output power of

generator g during time interval t. $R^{\mathrm{U}}_{g,t}/R^{\mathrm{D}}_{g,t}$ are the upward/downward reserves provided by generator g, respectively. k^0_g, k^1_g and k^2_g refer to the generation cost coefficients and q^{U}_g and q^{D}_g describe the reserve cost coefficients. Since the cost of WP is not counted in, the economic optimization will autonomously result in the increase in WP output power within the feasible range.

3.3.2. Constraints

- Power balance considering the reserve

$$\begin{cases} \sum\limits_{g=1}^{G} P^{\mathrm{G}}_{g,t} + \sum\limits_{w=1}^{N_{\mathrm{W}}} P^{\mathrm{W}}_{w,t} + \sum\limits_{g=1}^{G} R^{\mathrm{U}}_{g,t} + \sum\limits_{n=1}^{N} R^{\mathrm{ADN,U}}_{n,t} \geq \sum\limits_{n=1}^{N} p^{\mathrm{ADN}}_{n,t} \\ \sum\limits_{g=1}^{G} P^{\mathrm{G}}_{g,t} + \sum\limits_{w=1}^{N_{\mathrm{W}}} P^{\mathrm{W}}_{w,t} - \sum\limits_{g=1}^{G} R^{D}_{g,t} - \sum\limits_{n=1}^{N} R^{\mathrm{ADN,D}}_{n,t} \leq \sum\limits_{n=1}^{N} p^{\mathrm{ADN}}_{n,t} \end{cases} \tag{24}$$

where N_{W} is the number of wind farms and $P^{\mathrm{W}}_{w,t}$ is the output power of wind farm w during time interval t. N refers to the total number of ADNs. $R^{\mathrm{ADN,U}}_{n,t}/R^{\mathrm{ADN,D}}_{n,t}$ indicate the upward/downward FRPs supplied by the ADN, respectively. $R^{\mathrm{ADN,U}}_{n,t}/R^{\mathrm{ADN,D}}_{n,t}= 0$, if $P^{\mathrm{ADN,\ F}}_{n,t} < 0$.

- Generators

$$\begin{cases} P^{\mathrm{G}}_{g,t} + R^{\mathrm{U}}_{g,t} \leq P^{\mathrm{G,max}}_{g} \\ P^{\mathrm{G,min}}_{g} \leq P^{\mathrm{G}}_{g,t} - R^{\mathrm{D}}_{g,t} \\ \left(P^{\mathrm{G}}_{g,t+1} + R^{\mathrm{U}}_{g,t+1}\right) - \left(P^{\mathrm{G}}_{g,t} - R^{\mathrm{D}}_{i,t}\right) \leq r^{\mathrm{u}}_{g} \\ \left(P^{\mathrm{G}}_{g,t+1} - R^{\mathrm{D}}_{g,t+1}\right) - \left(P^{\mathrm{G}}_{g,t} + R^{\mathrm{U}}_{g,t}\right) \geq r^{\mathrm{d}}_{g} \\ R^{\mathrm{U}}_{g,t}, R^{\mathrm{D}}_{g,t} \geq 0 \\ P^{\mathrm{W}}_{w,t} \leq p^{\mathrm{wind}}_{w,t} \\ 0 \leq R^{\mathrm{ADN,U}}_{n,t} \leq p^{\mathrm{ADG}}_{n,t} - p^{\mathrm{ADN,min}}_{n,t} \\ 0 \leq R^{\mathrm{ADN,D}}_{n,t} \leq p^{\mathrm{ADN,max}}_{n,t} - p^{\mathrm{ADN}}_{n,t} \end{cases} \tag{25}$$

where $P^{\mathrm{G,max}}_{g}/P^{\mathrm{G,min}}_{g}$ are the maximum/minimum power of generator g, of which $r^{\mathrm{u}}_{g}/r^{\mathrm{d}}_{g}$ are the upward/downward reserves.

- Transmission line

$$\begin{cases} T^{\min}_{c} \leq G_{c-b} \sum\limits_{b=1}^{N_{\mathrm{B}}} \left[P^{\mathrm{G}}_{b,t} + P^{\mathrm{W}}_{b,t} + R^{\mathrm{U}}_{b,t} + R^{\mathrm{ADN,U}}_{b,t} - p^{\mathrm{ADN}}_{b,t}\right] \leq T^{\max}_{c} \\ T^{\min}_{c} \leq G_{c-b} \sum\limits_{b=1}^{N_{\mathrm{B}}} \left[P^{\mathrm{G}}_{b,t} + P^{\mathrm{W}}_{b,t} + R^{\mathrm{U}}_{b,t} - R^{\mathrm{ADN,D}}_{b,t} - p^{\mathrm{ADN}}_{b,t}\right] \leq T^{\max}_{c} \end{cases} \tag{26}$$

where $T^{\max}_{c}/T^{\min}_{c}$ are the maximum/minimum power of transmission line c. G_{c-b} is the transfer coefficient of power flow for line l to node b. N_{B} is the total number of nodes in the TG.

4. Solution Methods

4.1. A Solution Method for RO Models

This paper adopts the C&CG algorithm to solve the multi-level scheduling for the MG, ADN and TG, which are RO problems in nested form and have an NP-hard nature. The core idea of C&CG is to gradually approach the solution of RO through the iteration of the master problem (MP) and the sub problem (SP) [31]. For the sake of simplicity, let y be the first stage decision variables, concerning BS, FL and thermal generators, which need to

be determined in real time. Let x be the second stage variables that can be determined after the uncertain parameters are further clarified. x includes variables related to PV, WP and GT. Now we turn to the algorithm as follows:

1. Set UB = $+\infty$, LB = $-\infty$, $r = 0$ and $\Theta = \varnothing$.
2. Solve the following MP:

$$\begin{aligned} &\text{MP}: \min_{y,\eta}\left(c^T y + \eta\right) \\ &\text{s.t.}\begin{cases} Ay \geq d, y \in S_y \\ \eta \geq b^T x^l, x^l \in S_x, \forall l \in \Theta \\ Jx^l \geq h - Ey - Mu^l, \forall l \leq r \\ \eta \in R, S_y \in R_+^n, S_x \in R_+^m \end{cases} \end{aligned} \tag{27}$$

An optimal solution $(y_{r+1}^*, \eta_{r+1}^*, x^{1*}, x^{2*}, \cdots, x^{r*})$ is derived. Update LB = max $\left\{LB, c^T y_{r+1}^* + \eta_{r+1}^*\right\}$.

3. Solve the following SP under given y_{r+1}^*:

$$\begin{aligned} &\text{SP}: \psi\left(y_{r+1}^*\right) = \max_{u \in U} \min bx \\ &\text{s.t.}\begin{cases} Jx \geq h - Ey_{r+1}^* - Mu \\ x \in S_x \end{cases} \end{aligned} \tag{28}$$

Obtain the worst scene u_*^{r+1}, and update UB = $\min\left\{\text{UB}, c^T y_{r+1}^* + \psi(y_{r+1}^*)\right\}$.

4. If UB $-$ LB $\leq \varepsilon_0$, return y_{r+1}^* and terminate. Otherwise,

   if $\psi(y_{r+1}^*) < +\infty$, create variable x^{r+1} and add the following constraints:

$$\begin{cases} \eta \geq b^T x^{r+1} \\ Gx^{r+1} \geq h - Ey - Mu_*^{r+1} \end{cases} \tag{29}$$

   to MP. Update $r = r + 1$, $\Theta = \Theta \cup \{r + 1\}$ and go to step two.
   If $\psi(y_{r+1}^*) = +\infty$, create variable x^{r+1} and add the following constraints:

$$Gx^{r+1} \geq h - Ey - Mu_*^{r+1} \tag{30}$$

   Update $r = r + 1$, $\Theta = \Theta \cup \{r + 1\}$ and go to step two.

4.2. Iteration between ADN and MGs

As previously stated, the prices for FRPs are distributed to MGs from the ADN. After ROs, according to the prices, have been carried out in MGs, the results will be sent back to the ADN. Hence, the following iteration steps are designed:

1. Set the minimum/maximum prices $C_{\min}^{\text{FRP}}/C_{\max}^{\text{FRP}}$ for the FRP of the MG and send to each MG at the initial prices.
2. MGs conduct RO based on prices for the FRP, then upload the results ($p_{i,t}^{\text{MG,base}}$ and $p_{i,t}^{\text{MO,up}}/p_{i,t}^{\text{MO,down}}$) to the ADN.
3. The optimization is carried out in the ADN based on the results feedback from the MGs. The iteration will be terminated if one of the following two situations occurs:

$$\left|\sum_{t \in T}\left(p_{\text{root},t,m}^{\text{ADN,max}} - p_{\text{root},t,m}^{\text{ADN,min}}\right) - \sum_{t \in T}\left(p_{\text{root},t,m-1}^{\text{ADN,max}} - p_{\text{root},t,m-1}^{\text{ADN,min}}\right)\right| \leq \varepsilon_1 \tag{31}$$

or prices for FRPs in all the time intervals reach the maximum limit. Otherwise, ω_m and the prices for FRPs will be amended as follows and return to step two:

$$\begin{cases} C_{m+1}^{\text{FR}} = \min\left[C_{\max}^{\text{FR}}, C_m^{\text{FR}} \ln(1/m + e)\right] \\ \omega_{m+1} = \omega_m[1 - 1/(2 + \ln m)] \end{cases} \tag{32}$$

where $C_{t,m}^{\mathrm{FRP}}$ includes prices for both upward/downward FRPs.

4.3. The Overall Execution Process

Figure 4 displays the overall execution process for the multi-level scheduling of the MG, ADN and TG. First, the RO is run independently by each MG under the FRP prices and other initial conditions. The only variables that interacted in the iteration between the ADN and MGs are $p_{i,t}^{\mathrm{MG,base}}$ and $p_{i,t}^{\mathrm{MO,up}}/p_{i,t}^{\mathrm{MO,down}}$, of which signs can be used to judge whether the MG is flexible or uncertain. Then, each ADN carries out RO to determine if $p_{\mathrm{root},t}^{\mathrm{ADN}}$ is adjustable and the flexible/uncertain range. Finally, the unit commitment will be conducted in the TG, and the results will be fed back to the ADN.

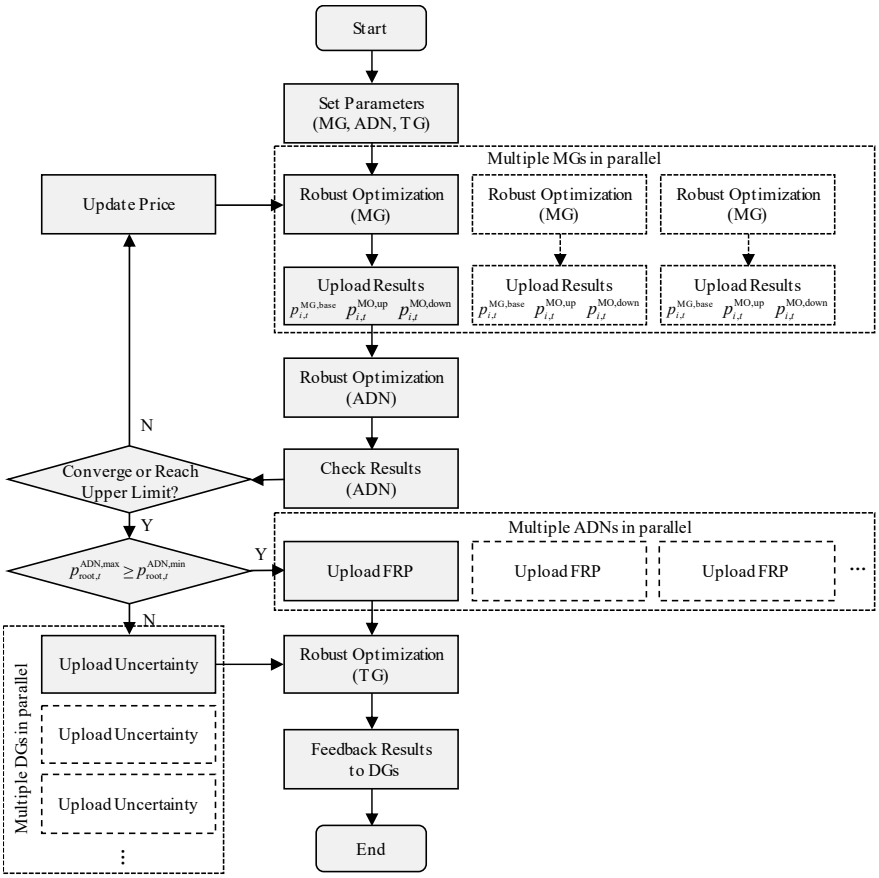


Figure 4. Execution process for multi-level scheduling.

5. Case Studies

In this section, the proposed RO models are validated in the multi-level power grid, depicted in Figure 5. There is a modified case-6 TG and two modified case-33 ADNs, of which parameters (line impedance, basic load, etc.) can be obtained from MATPOWER. MG1~MG4 are located in ADN1, and MG5~MG7 are located in ADN2. The elements in each MG are presented in the figure below. T = 4 h, Δt = 15 min and the optimizations start at 8:00. The convergence tolerance ε_0 and ε_1 are both set to 10^{-2}. The initial weight coefficient ω_1 is 0.5. The maximum load L in bus-5 of the TG is set to 220 MW. The detailed parameters and uncertain sets of the multi-level grid are provided in the Appendix A. Table 1 displays the time-of-use electricity prices for the MGs. The minimum/maximum prices for upward FRPs are 0.14/0.37 (USD/kW), and the minimum/ maximum prices for downward FRPs are 0.01/0.06 (USD/kW).

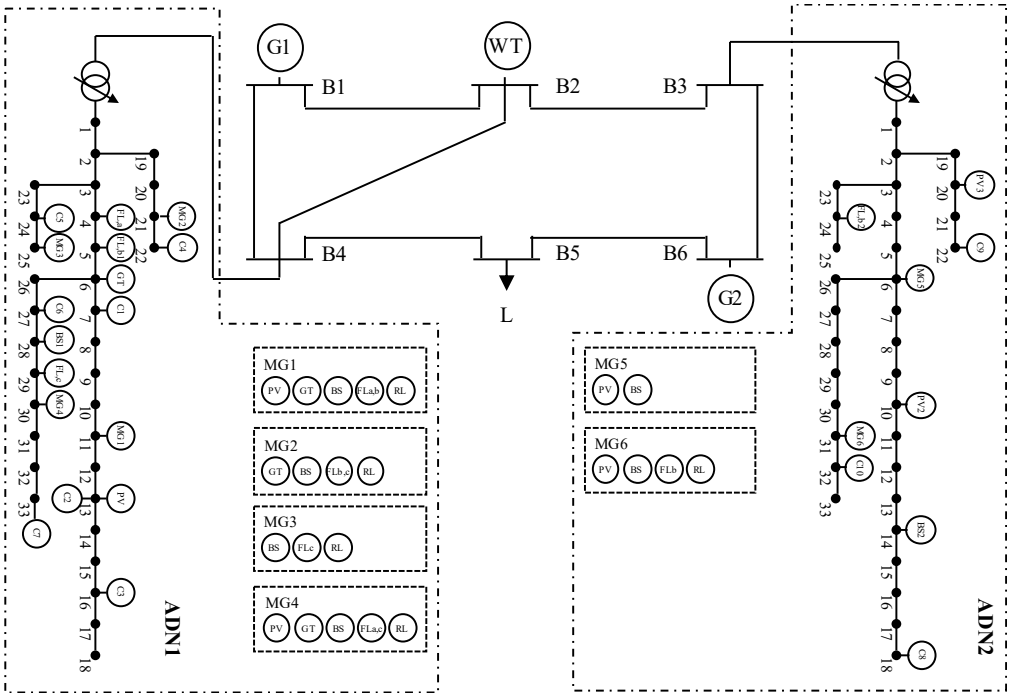


Figure 5. A modified multi-level power grid.

Table 1. Power purchase price of MG.

Time Intervals	8:00~12:00; 17:00~21:00	12:00~17:00; 21:00~24:00	0:00~8:00
$C_{i,t}^{MG,base}$(USD/kWh)	0.53	0.32	0.15

All the experiments were carried out on a personal computer with an Intel Core i7-9700 CPU and 32GB of RAM using MATLAB 2019a with MOSEK.

5.1. Flexibilities/Uncertainties of MGs and ADNs

The purpose of this section is to illustrate the results of proposed scheduling strategies on excavating the flexibilities and portraying the uncertainties of the ADN/MG. The results of RO optimizations of MGs are displayed in Figure 6, including the base powers and the power boundaries considering flexibilities/uncertainties. MG2, MG3 and MG5 converge because the optimization results are stable, while MG1, MG4 and MG6 stop iterating because the FRP price limits are reached. MG1, MG2 and MG4 sell FRPs to the ADN: when the MG reduces its power, it provides an upward FRP to the ADN. On the other hand, when the MG increases its power, a downward FRP is achieved by the ADN. The adjustable ranges reach 69.03, 18.96 and 16.82% of their base powers, respectively. These results may be due to the abundance of their internal resources. MG5, which only has PV and BS, mainly has a downward FRP to be exploited. MG3 has to purchase an FRP from the ADN since it contains fewer flexible resources, which cannot cover the uncertainties with rather big basic loads. However, the RO reduces its demand for outside an FRP to lower than 17.25% of its basic power. The situation of MG6 is a bit special. Flexibilities and uncertainties simultaneously exist, but the controllable and uncontrollable ranges are both small, which are less than 2.25% of its basic power.

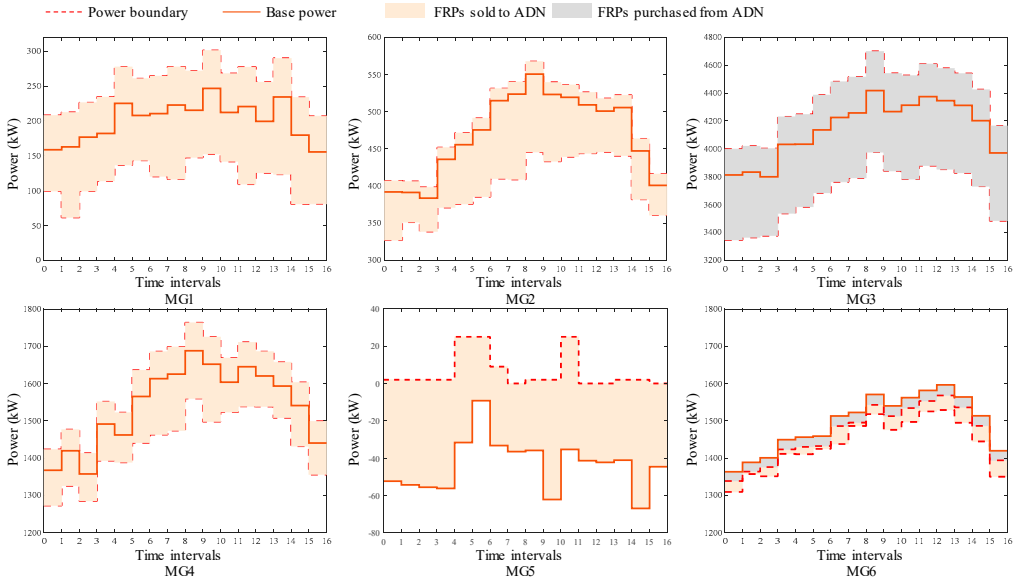


Figure 6. Optimization results of MGs.

ADN1 and ADN2 converged after 11 and 13 iterations, respectively. The flexible/uncertain power ranges of ADN1 and ADN2 are shown in Figure 7. The robust minimum values are smaller than the robust maximum values of power in the ADN1 root node. This means that ADN1 can provide the TG with a flexible power range of about 10 MW after overcoming its uncertainties. However, the flexible resources in the ADN2 are not enough to offset the influence of internal uncertainties on the optimization results, resulting in an uncertain range (about 3% of its own basic power) to the TG. MG1, MG4~MG6, ADN1 and ADN2 contain REPG, of which the consumption rates are above 95% after optimization.

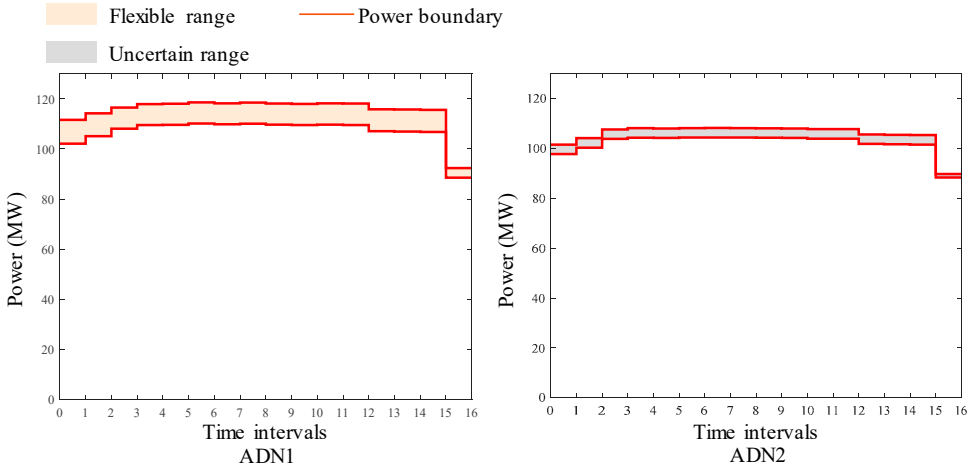
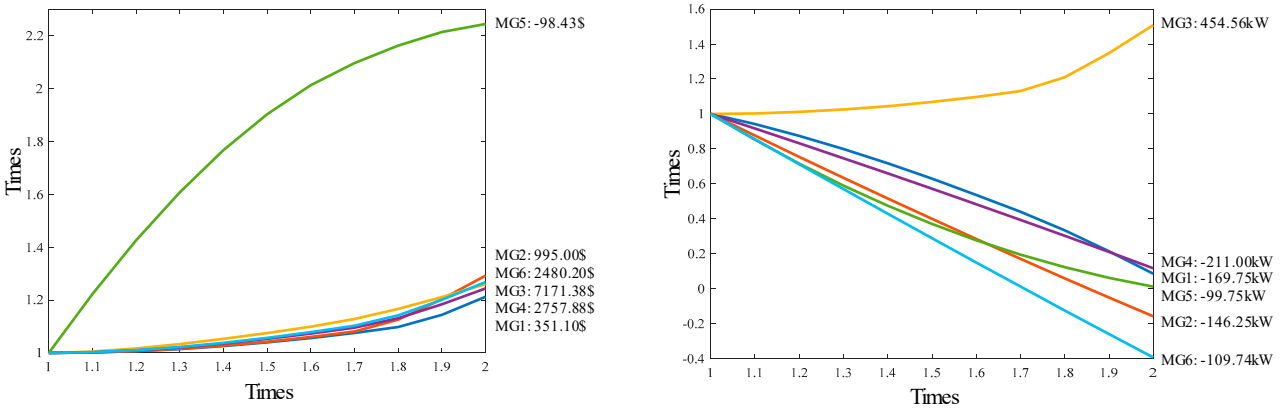


Figure 7. Optimization results of ADNs.

5.2. Sensitivity Analysis to Price

To assess the effect of electricity purchase prices on the optimal dispatch, experiments were carried out under proportionally changed prices. Figure 8a displays the impact of electricity prices on the operating costs of MGs, of which the initial values are marked on the right. Additionally, the coordinate on the horizontal axis represents the multiple of the current price relative to the initial price. Since MG1~4 and MG6 are all purchasers of electricity, the operational costs rise along with electricity prices. The growth rate of operational expense increases with the increase in the electricity price as well. A possible explanation for this might be that the flexible resources have reached their output limitation

and cannot alleviate the impact of higher electricity prices further. MG5 sells electricity to ADN2. Its operating income rises significantly with the electricity price. Figure 8b shows the influence of electricity prices on the moderate demand of MGs for an outside FRP ($\sum_{t\in T}(p_{i,t}^{\mathrm{MO,up}} + p_{i,t}^{\mathrm{MO,down}})/T$) during the scheduling period, and the initial values are also marked on the right. The average demands of MG1~2 and MG4~6 under the initial electricity price are less than 0, while the demand of MG5 is greater than 0. The demands for an external FRP increase and the signs of MG2 and MG6 are changed due to the growth of electricity price. These results are likely to be related to the flexible resources that are employed to reduce the growth of operational costs under high electricity prices, resulting in the decline of flexibilities.

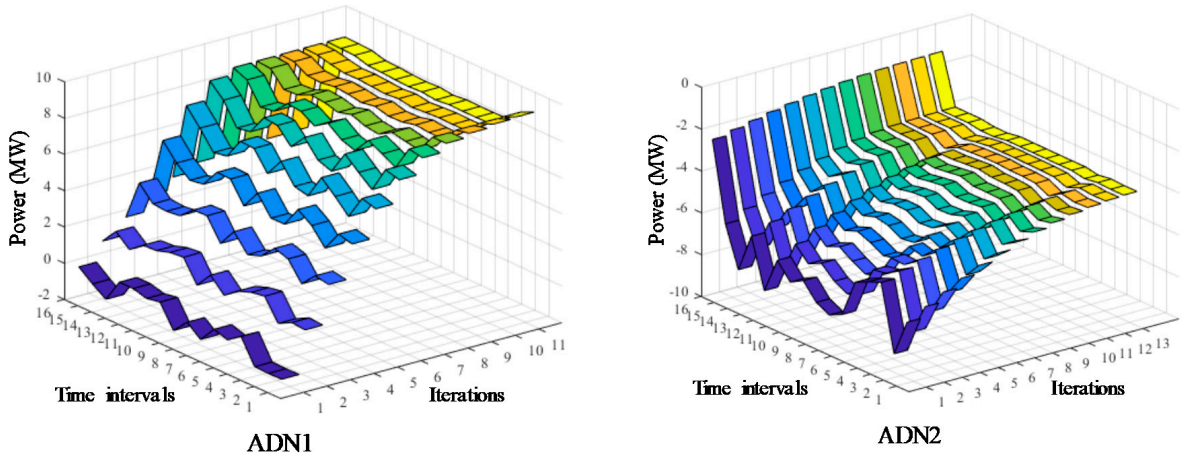


(**a**) influence on operating costs (**b**) influence on outside FRP

Figure 8. The influence of electricity price on dispatching results of MGs.

The $P_{\mathrm{root},t}^{\mathrm{ADN,F}}$ and network losses of ADN1 and ADN2 in different iterations are presented in Figure 9. Eleven and thirteen iterations are performed on ADN1 and ADN2, respectively. The prices for an FRP in ADN2 reach the upper limitations. $P_{\mathrm{root},t}^{\mathrm{ADN,F}}$ of ADN1 are lower than 0 under the initial prices for an FRP and eventually, converge to values above 0 with the growth of prices. The $P_{\mathrm{root},t}^{\mathrm{ADN,F}}$ of ADN2 are still below 0 under the maximum price for an FRP; however, the increases in charges for an FRP reduce its uncertainties. As shown in Figure 10, owing to the rise of the weight coefficient, the convergence of the network losses is accelerated, and the minimum values are achieved after five to six iterations.

Table 2 compares the optimizations of ADNs in different limit ranges for FRP prices. Since the iteration of ADN1 is terminated due to the trigger of the condition that the changes of powers are extremely insignificant, the changes of the price limit range do not affect the scheduling results of ADN1. However, the lower minimum price brings a wider iteration range, which leads to the increase in the calculation time. The rise of the maximum price results in a restricted improvement of ADN2 scheduling effects but also brings a higher computational burden that may limit online applications.



(**a**) iterations of ADN1 (**b**) iterations of ADN2

Figure 9. $P_{\text{root},t}^{\text{ADN, F}}$ in different iterations.

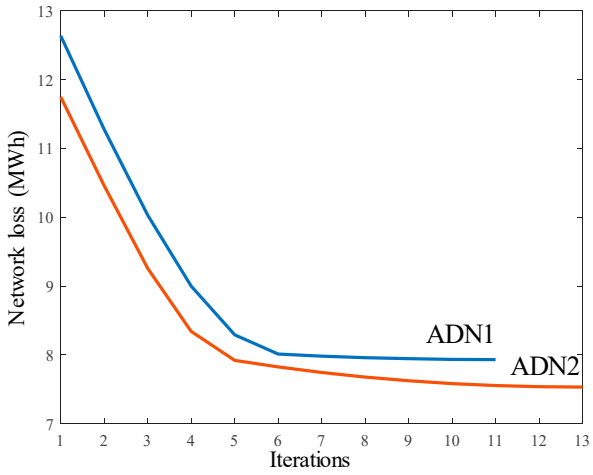


Figure 10. Network losses in different iterations.

Table 2. Comparison of optimizations under different price ranges.

	Price Ranges for FRP					
$C^{\text{MO,up}} \in$	[0.05, 0.37]		[0.14, 0.37]		[0.14, 1.00]	
$C^{\text{MO,down}} \in$	[0.01, 0.06]		[0.01, 0.06]		[0.01, 0.06]	
	ADN1	ADN2	ADN1	ADN2	ADN1	ADN2
Iterations	179	208	11	13	11	69
Calculation time(s)	419.93	487.34	30.76	37.84	30.76	161.39
$\sum_{t\in\text{T}} P_{\text{root},t}^{\text{F}}$(kW)	133.32	−58.65	133.32	−58.65	133.32	−53.31
Network losses (MWh)	7.93	7.53	7.93	7.53	7.93	7.12

5.3. Effectiveness for TG

The purpose of the experiments below are to verify the application effects of the proposed dispatching strategy for the TG:

Case one: the strategy proposed in this paper is adopted in both MGs and ADNs. The RO in the TG is conducted after ADN1 uploads the controllable ranges, while ADN2 reports the uncertain ranges to the TG.

Case two: the strategy proposed in this paper is not employed in MGs and ADNs. The RO in the TG is carried out assuming that the powers in the root nodes of ADN1 and ADN2 fluctuate within 10% of their base values.

Table 3 displays the comparison between optimization results of case one and case two in the TG:

Table 3. Comparison of optimization results in TG.

	Case 1	**Case 2**
Operating cost of TG (USD)	12,862.64	13,724.44
The consumption rate of WP (%)	95.87%	89.66%

For the TG, the application of the proposed strategy can reduce the need for generator reserve. The consumption rate of WP is improved while the operating cost of the TG declines.

6. Conclusions

This study set out to exploit the flexibilities of a multi-level power grid, which can play a crucial role in dealing with the uncertainties caused by the widely developed REPGs. A multi-level scheduling framework for the MG, ADN and TG has been established. Unified models for flexibilities/uncertainties of the MG and ADN have been developed based on RO. The iterations between the ADN and MGs have been carried out to maximize the utilization of flexibilities within different participants considering the economic costs. These studies provide new insights into awareness and improvement strategies for the flexibilities of multi-level scheduling. Based on the proposed methods, the ADN's flexibilities were expanded while the uncertainties were curtailed, supplying new resources for the unit commitment with REPGs in the TG.

Simulations on cases including a modified 6-bus TG, two modified 33-bus ADNs and several MGs have been carried out to verify the effectiveness of the strategy proposed in this paper. This study had identified that when the ADN had sufficient flexible resources, the robust minimum powers at the root node were less than the robust maximum values, which brought controllable ranges for the TG. Otherwise, the ADN should be treated as uncertain loads toward the TG. The results demonstrated that the awareness of flexibilities and reduction in uncertainties in the ADNs are favorable to the unit commitment for the TG. The operating cost had decreased by 6.28%, and the consumption rate of WP had risen by 6.21%. The comparative examples have shown that high electricity prices may limit flexibility. Moreover, reasonable price ranges for FRPs are suggested to be employed to balance calculation time with optimization results. Further research might explore the combination of scenario and robust methods to reduce the conservatism, and a more practical price mechanism needs to be investigated.

Author Contributions: Conceptualization, Z.Z. and Z.C.; methodology, Z.Z.; software, Z.Z.; validation, Q.Z., and P.D.; investigation, Z.Z.; resources, Q.Z.; writing—original draft preparation, Z.Z.; writing—review and editing, P.D.; supervision, Z.C. All authors have read and agreed to the published version of the manuscript.

Funding: This research was funded by the State Grid Technology Project under Grant 5108-202018026A-0-0-00.

Institutional Review Board Statement: Not applicable.

Informed Consent Statement: Not applicable.

Data Availability Statement: The data presented in this study are available on request from the corresponding author. The data are not publicly available due to business secret.

Conflicts of Interest: Zhong Chen has received research grants from State Grid Corporation. Qi Zhao is employee of State Grid Corporation. The authors declare no conflict of interest.

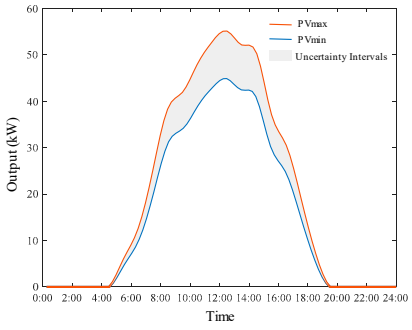
Abbreviations

Abbreviations	
ADN	Active Distribution Network
BS	Battery Storage
FRP	Flexible Ramping Product
FL	Flexible Load
GT	Gas Turbine
MG	Micro-Grid
PV	Photovoltaics
REPG	Renewable Energy Power Generation
RL	Regular Load
RO	Robust Optimization
TG	Transmission Grid
WP	Wind Power
Sets and indices	
i	Index for MG
j, k, l	Index for the node of ADN
m, r	Index for iteration
n	Index for ADN
g	Index for thermal generator
h	Index for operating point of reducible load
w	Index for wind farms
b	Index for the node of TG
c	Index for the line of TG
$\boldsymbol{P}^{\mathrm{MG}}$	Uncertain budget of MG power
$\boldsymbol{P}^{\mathrm{L}}$	Uncertain budget of RL
$\boldsymbol{P}^{PV}$	Uncertain budget of PV output
$\boldsymbol{P}^{\mathrm{wind}}$	Uncertain budget of WP output
$\boldsymbol{P}^{\mathrm{P,\ ADN}}$	Uncertain budget of parameters in ADN
P^{ADN}	Uncertain budget of ADN power
t	Index for time intervals
T	Number of time intervals
$u(\cdot)/v(\cdot)$	Set of end/head nodes
Parameters	
$C^{\mathrm{MG,base}}$	The unit power purchase price for MG
$C^{\mathrm{MG,B}}$	The unit power cost of BS
$C^{\mathrm{MO,up}}/C^{\mathrm{MO,down}}$	The unit price for upward/downward FRP
$C^{x,\mathrm{GT}}/\ B^{x,\mathrm{GT}}$	Fixed/variable cost of GT
Δt	Length of time interval
$P^{x,\ \mathrm{BC}}_{\max}/P^{x,\ \mathrm{BC}}_{\min}$	Maximum/minimum power of BS charging
$P^{x,\ \mathrm{BD}}_{\max}/P^{x,\ \mathrm{BD}}_{\min}$	Maximum/minimum power of BS discharging
$E^{x,\ \mathrm{B}}_{t_0}$	Energy in BS at the initial moment
$E^{x,\mathrm{B}}_{\max}\ /E^{x,\mathrm{B}}_{\min}$	Maximum/minimum energy of BS
$P^{x,\ \mathrm{GT}}_{\max}/P^{x,\ \mathrm{GT}}_{\min}$	Maximum/minimum power of GT
$\Delta P^{x,\ \mathrm{GT}}$	Power change limitation between time intervals of GT
$T^{x,\ \mathrm{GT}}_{\mathrm{run,min}}/T^{x,\ \mathrm{GT}}_{\mathrm{down,min}}$	Minimum on/off time of GT
$[\alpha^{x,\ \mathrm{FL},\ y}, \beta^{x,\ \mathrm{FL},\ y}]$	The schedulable time interval of FL
$E^{x,\ \mathrm{FL,\ b}}_{\max}/E^{x,\ \mathrm{FL,\ b}}_{\min}$	Maximum/minimum energy absorbed by the interruptible load
n_{c}	Number of discrete operating points of reducible load
$Q^{\mathrm{com}}_{\max}/Q^{\mathrm{com}}_{\min}$	Maximum/minimum reactive power of compensation device
$k^0_g/k^1_g/k^2_g$	Generation cost coefficient
$q^{\mathrm{U}}_g/q^{\mathrm{D}}_g$	Reserve cost coefficient

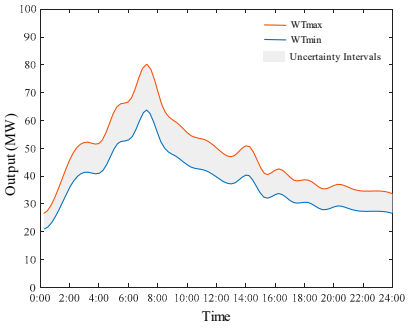
N	Number of ADNs
N_{W}	Number of wind farms
N_{B}	Number of nodes in TG
$T^{\max}/T^{\min}$	Maximum/minimum power of transmission line
G_{c-b}	Transfer coefficient of power flow for the line to node
$\varepsilon_0/\varepsilon_1$	Convergence criterion
C^{FRP}	Price for upward/downward FRP.
Variables	
$p^{\mathrm{MG,base}}$	Power from ADN to MG
$p^{\mathrm{MG},\,x}$	Power of PV, BS, GT, and FL inside MG
$p^{\mathrm{MG,up}}/p^{\mathrm{MG,down}}$	Upward/downward FRP to cover the uncertainties of MG
$p^{\mathrm{MI,up}}/p^{\mathrm{MI,down}}$	Upward/downward FRP obtained inside MG
$p^{\mathrm{MO,up}}/p^{\mathrm{MO,down}}$	Upward/downward FRP transactions between MG and ADN
$p^{x,\,\mathrm{BC}}/p^{x,\,\mathrm{BD}}$	Charge/discharge power of BS
$u^{x,\,\mathrm{GT}}$	Operating status of GT
$p^{\mathrm{MG},\,x,\mathrm{up}}/p^{\mathrm{MG},\,x,\mathrm{down}}$	Upward/downward FRP of PV, BS, GT, and FL inside MG
$u^{x,\,\mathrm{BC}}/u^{x,\,\mathrm{BD}}$	Charging/discharging state of BS
$E^{x,\,\mathrm{B,\,up}}/E^{x,\,\mathrm{B,\,down}}$	Energy in BS considering upward/downward flexibility
$s^{x,\,\mathrm{BCD}}/s^{x,\,\mathrm{BDC}}$	Whether BS is switched from charging/discharging state to discharging/charging state
$u^{x,\,\mathrm{FL},\,y}/s^{x,\,\mathrm{FL},\,y}$	Operating/starting state of FL
U	Square of voltage amplitude
L	Square of current amplitude
$p^{\mathrm{ADN}}_{\mathrm{root}}$	Power of ADN root node
$P^{\mathrm{ADN,\,F}}$	Flexibility of ADN
P^{G}	The output power of the generator
$R^{\mathrm{U}}/R^{\mathrm{D}}$	Upward/downward reserve of generator

Appendix A

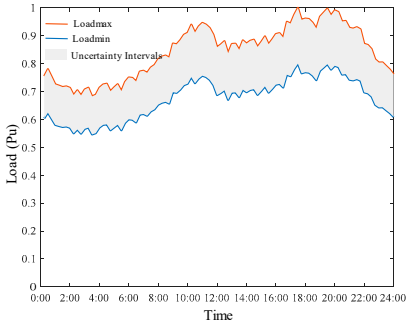
Uncertainties in an MG, an DG and a TG



(**a**) uncertainties of PV



(**b**) uncertainties of WT



(**c**) uncertainties of Load

Figure A1. Interval forecast of PV output, WT output and load (per unit).

Table A1. Parameters of energy storage system (MG).

$P_{\max}^{\mathrm{MG,BC}}$	$P_{\min}^{\mathrm{MG,BC}}$	$P_{\max}^{\mathrm{MG,BD}}$	$P_{\min}^{\mathrm{MG,BD}}$	$E_{\max}^{\mathrm{MG,B}}$	$E_{\min}^{\mathrm{MG,B}}$	$E_{t_0}^{\mathrm{MG,B}}$	$C_i^{\mathrm{MG,B}}$
25 kW	2 kW	20 kW	2 kW	50 kWh	5 kWh	20 kWh	USD 0.02/kWh

Table A2. Parameters of gas turbine (MG).

$P_{\max}^{\mathrm{MG,GT}}$	$P_{\min}^{\mathrm{MG,GT}}$	$\Delta P^{\mathrm{MG,GT}}$	$T_{\mathrm{run,min}}^{\mathrm{MG,GT}}$	$T_{\mathrm{down,min}}^{\mathrm{MG,GT}}$	$C^{\mathrm{MG,GT}}$	$B^{\mathrm{MG,GT}}$
300 kW	50 kW	50 kW	45 min	45 min	USD 0.6/kWh	USD 8

Table A3. Parameters of flexible load (MG, in 96 intervals of 24 h).

	α^{MG}	β^{MG}	$P^{\mathrm{MG,FL}}$**(kW)**	$T^{\mathrm{MG,FL,a}}$	$E_{\max}^{\mathrm{MG,FL,b}}$**(kWh)**	$E_{\min}^{\mathrm{MG,FL,b}}$**(kWh)**
Transferable load (FL,a)	33	49	$P^{\mathrm{MG,FL,a}} = 20$	6	-	-
Interruptible load (FL,b)	36	52	$P_{\max}^{\mathrm{MG,FL,b}} = 25, P_{\min}^{\mathrm{MG,FL,b}} = 5$	-	70	40
Reduce-able load (FL,c)	38	43	$\boldsymbol{P}_k^{\mathrm{MG,FL,c}} = [10, 15, 21, 27, 50]$	-	-	-

Table A4. Parameters of reactive power compensation device.

MVar	**C1**	**C2**	**C3**	**C4**	**C5**	**C6**	**C7**	**C8**	**C9**	**C10**
$-Q_{i,\min}^{\mathrm{com}}$	1.5	1.5	1.6	1.6	1.6	1.2	1.0	1.5	1.5	1.6
$Q_{i,\max}^{\mathrm{com}}$	0.5	0.5	0.5	0.5	0.5	0.5	0.5	0.5	0.5	0.5

Table A5. Parameters of energy storage system (ADN).

$P_{\mathbf{max}}^{\mathbf{ADN,BC}}$	$P_{\mathbf{min}}^{\mathbf{ADN,BC}}$	$P_{\mathbf{max}}^{\mathbf{ADN,BD}}$	$P_{\mathbf{min}}^{\mathbf{ADN,BD}}$	$E_{\mathbf{max}}^{\mathbf{ADN,B}}$	$E_{\mathbf{min}}^{\mathbf{ADN,B}}$	$E_{t_0}^{\mathbf{ADN,B}}$	$C_i^{\mathbf{ADN,B}}$
80 kW	5 kW	40 kW	5 kW	100 kWh	10 kWh	40 kWh	USD 0.02/kWh

Table A6. Parameters of gas turbine (ADN).

$P_{\max}^{\mathrm{ADN,GT}}$	$P_{\min}^{\mathrm{ADN,GT}}$	$\Delta P^{\mathrm{ADN,GT}}$	$T_{\mathrm{run,min}}^{\mathrm{ADN,GT}}$	$T_{\mathrm{down,min}}^{\mathrm{ADN,GT}}$	$C^{\mathrm{ADN,GT}}$	$B^{\mathrm{ADN,GT}}$
5000 kW	60 kW	60 kW	60 min	60 min	USD 0.5/kWh	USD 10

Table A7. Parameters of flexible load (ADN, in 96 intervals of 24h).

	α^{ADN}	β^{ADN}	$P^{\mathrm{ADN,FL}}$**(kW)**	$T^{\mathrm{ADN,FL,a}}$	$E_{\max}^{\mathrm{ADN,FL,b}}$**(kWh)**	$E_{\min}^{\mathrm{ADN,FL,b}}$**(kWh)**
Transferable load (FL,a)	27	48	$P^{\mathrm{ADN,FL,a}} = 60$	6	-	-
Interruptible load (FL,b)	30	54	$P_{\max}^{\mathrm{ADN,FL,b}} = 60$, $P_{\min}^{\mathrm{ADN,FL,b}} = 20$	-	150	80
Reduce-able load (FL,c)	40	46	$\boldsymbol{P}_k^{\mathrm{ADN,FL,c}} = [20, 30, 42, 54, 80]$	-	-	-

Table A8. Generator data.

G	$P^{\mathrm{G,max}}$**(MW)**	$P^{\mathrm{G,min}}$**(MW)**	k^0**(USD)**	k^1**(USD/MWh)**	k^2**(USD/MWh2)**	q^{U}**(USD/MW)**	q^{D}**(USD/MW)**
1	40	220	50	7	0.03	3.5	3
2	0	25	55	8	0.05	4	2

Table A9. Network information.

From Bus	To Bus	X(pu)	Flow Limit (MW)
1	2	0.170	200
1	4	0.258	200
2	3	0.037	190
2	4	0.197	200
3	6	0.018	180
4	5	0.037	190
5	6	0.140	180

References

1. Hansen, K.; Mathiesen, B.V.; Skov, I.R. Full energy system transition towards 100% renewable energy in Germany in 2050. *Renew. Sustain. Energy Rev.* **2019**, *102*, 1–13. [CrossRef]
2. Kang, C.Q.; Yao, L.Z. Key scientific issues and theoretical research framework for power systems with high proportion of renewable energy. *Autom. Electr. Power Syst.* **2017**, *41*, 2–11.
3. Yang, Y.; Bao, M.; Ding, Y.; Jia, H.; Lin, Z.; Xue, Y. Impact of down spinning reserve on operation reliability of power systems. *J. Mod. Power Syst. Clean Energy* **2020**, *8*, 709–718. [CrossRef]
4. Gerard, H.; Puente, E.I.R.; Six, D. Coordination between transmission and distribution system operators in the electricity sector: A conceptual framework. *Util. Policy* **2018**, *50*, 40–48. [CrossRef]
5. Ji, X.Q.; Zhang, Y.M.; Han, X.S.; Ye, P.F.; Xu, B.; Yu, Y.J. Multi-level interactive unit commitment of regional power system. *Int. J. Electr. Power Energy Syst.* **2021**, *125*, 106464. [CrossRef]
6. Adam, H.; Yael, P.; Josep, G. Microgrids: A review of technologies, key drivers, and outstanding issues. *Renew. Sustain. Energy Rev.* **2018**, *90*, 402–411.
7. Bornapour, M.; Hooshmand, R.; Parastegari, M. An efficient scenario-based stochastic programming method for optimal scheduling of CHP-PEMFC, WT, PV and hydrogen storage units. *Renew. Energy* **2018**, *130*, 1049–1066. [CrossRef]
8. Cominesi, S.R.; Farina, M.; Giulioni, L.; Picasso, B.; Scattolini, R. A two-layer stochastic model predictive control scheme for microgrids. *IEEE Trans. Control. Syst. Technol.* **2018**, *26*, 1–13. [CrossRef]
9. Zhe, L.; Hu, Z.C.; Song, Y.H. Convex relaxation for optimal power flow problem: A recent review. *Proc. Chin. Soc. Electr. Eng.* **2019**, *39*, 3717–3727.
10. Farivar, M.; Low, S.H. Branch flow model: Relaxations and convexification—Part I. *IEEE Trans. Power Syst.* **2013**, *28*, 2554–2564. [CrossRef]
11. Tacbatabaee, S.; Mortazavi, S.S.; Niknam, T. Stochastic scheduling of local distribution systems considering high penetration of plug-in electric vehicles and renewable energy sources. *Energy* **2017**, *121*, 480–490. [CrossRef]
12. Dong, L.; Li, J.; Pu, T.J.; Chen, N.S. Distributionally robust optimization model of active distribution network considering uncertainties of source and load. *J. Mod. Power Syst. Clean Energy* **2019**, *7*, 1585–1595. [CrossRef]
13. Tuohy, A.; Meibom, P.; Denny, E.; O'Malley, M. Unit commitment for systems with significant wind penetration. *IEEE Trans. Power Syst.* **2009**, *24*, 592–601. [CrossRef]
14. Papavasiliou, A.; Oren, S.S.; O'Neill, R.P. Reserve requirements for wind power integration: A scenario-based stochastic programming framework. *IEEE Trans. Power Syst.* **2011**, *26*, 2197–2206. [CrossRef]
15. Wang, Q.F.; Guan, Y.P.; Wang, J.H. A chance-constrained two-stage stochastic program for unit commitment with uncertain wind power output. *IEEE Trans. Power Syst.* **2012**, *27*, 206–215. [CrossRef]
16. Kargarian, A.; Fu, Y. Systems of Systems Based Security-Constrained Unit Commitment Incorporating Active Distribution Grids. *IEEE Trans. Power Syst.* **2014**, *29*, 2489–2497. [CrossRef]
17. Wang, Y.W.; Tang, L.; Yang, Y.J.; Sun, W.; Zhao, H.R. A stochastic-robust coordinated optimization model for CCHP micro-grid considering multi-energy operation and power trading with electricity markets under uncertainties. *Energy* **2020**, *198*, 1–19. [CrossRef]
18. Zhao, C.Y.; Wang, J.H.; Watson, J.-P.; Guan, Y.P. Multi-Stage Robust Unit Commitment Considering Wind and Demand Response Uncertainties. *IEEE Trans. Power Syst.* **2013**, *28*, 2708–2717. [CrossRef]
19. Alavi, S.A.; Masoud, A.A.; Aliakbar-Golkar, M. Optimal probabilistic energy management in a typical micro-grid based-on robust optimization and point estimate method. *Energy Convers. Manag.* **2015**, *95*, 314–325. [CrossRef]
20. Lin, Z.J.; Chen, H.Y.; Wu, Q.W.; Huang, J.P.; Li, M.S.; Ji, T.Y. A data-adaptive robust unit commitment model considering high penetration of wind power generation and its enhanced uncertainty set. *Int. J. Electr. Power Energy Syst.* **2021**, *129*, 1–14. [CrossRef]
21. Bahramara, S.; Mazza, A.; Chicco, G.; Shafie-khah, M.; Catalão, J.P. Comprehensive review on the decision-making frameworks referring to the distribution network operation problem in the presence of distributed energy resources and microgrids. *Int. J. Electr. Power Energy Syst.* **2020**, *115*, 105466. [CrossRef]
22. Mohiti, M.; Monsef, H.; Anvari-Moghaddam, A.; Guerrero, J.; Lesani, H. A decentralized robust model for optimal operation of distribution companies with private microgrids. *Int. J. Electr. Power Energy Syst.* **2019**, *106*, 105–123. [CrossRef]

23. Zhang, X.; Wang, H.T. Optimal dispatch method of transmission and distribution coordination for power systems with high proportion of renewable energy. *Autom. Electr. Power Syst.* **2019**, *43*, 67–75, 115.
24. Wang, L.L.; Zhu, Z.; Jiang, C.W.; Li, Z.Y. Bi-level robust optimization for distribution system with multiple microgrids considering uncertainty distribution locational marginal price. *IEEE Trans. Smart Grid.* **2021**, *12*, 1104–1117. [CrossRef]
25. Li, J.; Liu, F.; Li, Z.; Shao, C.; Liu, X. Grid-side flexibility of power systems in integrating large-scale renewable generations: A critical review on concepts, formulations and solution approaches. *Renew. Sustain. Energy Rev.* **2018**, *93*, 272–284. [CrossRef]
26. Ji, H.; Wang, C.; Li, P.; Song, G.; Yu, H.; Wu, J. Quantified analysis method for operational flexibility of active distribution networks with high penetration of distributed generators. *Appl. Energy* **2019**, *239*, 706–714. [CrossRef]
27. Heussen, K.; Koch, S.; Ulbig, A.; Andersson, G. Unified System-Level Modeling of Intermittent Renewable Energy Sources and Energy Storage for Power System Operation. *IEEE Syst. J.* **2012**, *6*, 140–151. [CrossRef]
28. Kalantar-Neyestanaki, M.; Sossan, F.; Bozorg, M.; Cherkaoui, R. Characterizing the Reserve Provision Capability Area of Active Distribution Networks: A Linear Robust Optimization Method. *IEEE Trans. Smart Grid.* **2020**, *11*, 2464–2475. [CrossRef]
29. Oikonomou, K.; Parvania, M.; Khatami, R. Deliverable Energy Flexibility Scheduling for Active Distribution Networks. *IEEE Trans. Smart Grid.* **2020**, *11*, 655–664. [CrossRef]
30. Tu, J.; Zhou, M.; Song, X.; Luan, K.; Li, Y. Research on Incentive Mechanism and Optimal Power Consumption Strategy for Residential Users' Participation in Peak Shaving of Power Grid. *Power Syst. Technol.* **2019**, *43*, 443–453.
31. Zeng, B.; Zhao, L. Solving Two-stage Robust Optimization Problems by a Constraint-and-Column Generation Method. *Oper. Res. Lett.* **2013**, *41*, 457–461. [CrossRef]